

# Copper-Binding Peptides Attenuate Microglia Inflammation through Suppression of NF- $\kappa$ B Pathway

Maria Elisa Caetano-Silva, Laurie A. Rund, Mario Vailati-Riboni, Maria Teresa Bertoldo Pacheco, and Rodney W. Johnson\*

**Scope:** Activation of microglia, the resident immune cells of the central nervous system, has been related to the etiology and progression of neurodegenerative diseases; thus, finding novel approaches to suppress the neuroinflammatory process is of utmost relevance.

**Methods and Results:** The anti-inflammatory activity of whey Cu-, Fe-, and Zn-binding peptides and their possible underlying mechanism of action were evaluated in microglia. Whey metal-binding peptides decreased nitric oxide production and tumor necrosis factor  $\alpha$  (TNF- $\alpha$ ) at mRNA and protein levels by stimulated BV-2 microglia in comparison to the control with no peptide treatment. The hydrophobicity, specific sequences, and possible synergistic effects seem to play a role. Cu-binding peptides (Cu-bp) presented anti-inflammatory activity both in BV-2 and primary microglia cultures. These peptides exert their action by suppressing nuclear factor kappa B (NF- $\kappa$ B) pathway since nuclear translocation of NF- $\kappa$ B p65 is decreased by roughly 30% upon Cu-bp treatment. Specific sequences identified in Cu-bp showed high affinity to bind NF- $\kappa$ B p65 by molecular docking (up to  $-8.8$  kcal mol $^{-1}$ ), corroborating the immunofluorescence studies.

**Conclusion:** Cu-bp represent food-derived peptides that may be useful for neuroprotective purposes. Chelation of copper excess in the CNS and the bioavailability of such peptides, as well as their behavior in *in vivo* models, deserve further research for future applications.

of brain homeostasis.<sup>[3]</sup> Microglia can transit from surveillance mode to activation mode when the brain homeostasis is somehow threatened, under events such as infection, trauma, and ischemia.<sup>[4]</sup> Also, the normal process of aging can tip microglia towards a pro-inflammatory phenotype that is hyperresponsive to inflammatory stimuli. This results in a significant increase in neuroinflammation,<sup>[1,5]</sup> with excessive release of inflammatory mediators, such as nitric oxide (NO), oxygen radicals, and pro-inflammatory cytokines.<sup>[6-8]</sup>

Chronic neuroinflammation has been associated with the onset and progression of neurodegenerative diseases, including Alzheimer's disease (AD), Parkinson's disease, and multiple sclerosis,<sup>[9]</sup> and microglia have been considered a promising pharmacological target for several diseases.<sup>[10]</sup> Finding compounds that can regulate microglia function in the senescent brain to decrease neurotoxic inflammatory mediators is of utmost importance. This can contribute to developing therapeutic treatments to prevent or delay progression of neurodegenerative diseases.

Oxidative stress has been related to chronic inflammation in neurodegenerative diseases<sup>[11]</sup> since the reactive oxygen species (ROS) and inflammation stimulate each other, causing a vicious cycle.<sup>[12]</sup> Among the number of factors that can contribute to the formation of oxygen and nitrogen reactive species (ROS/RNS) are the elevated levels of redox-active transition metals in the brain, which can elicit necrotic neuronal death as a result of the production of these toxic species.<sup>[13]</sup> Metals ions such as Cu, Zn, and Fe, are highly concentrated in the brain and their distribution is heterogeneous in the different areas of the brain. Cu brain concentrations range from 2.9 to 5.9  $\mu\text{g g}^{-1}$ <sup>[14]</sup> and glial cells are enriched in Cu as compared to neurons.<sup>[15]</sup> The concentration of Zn and Fe in the normal brain range from 19.8 to 25.4 and 13.6–24.2  $\mu\text{g g}^{-1}$ , respectively.

In the AD brain, Cu ions are related to the free radical formation via Fenton reaction,<sup>[16]</sup> and the elevation of Cu levels in brains from AD patients has been correlated with tissue oxidative damage.<sup>[17]</sup> Also, microglia are involved in Fe homeostasis in the brain, and the release of pro-inflammatory cytokines and

## 1. Introduction

Microglia are mononuclear myeloid cells present in the brain that are crucial in immune surveillance, mediating immune responses and inflammatory processes in this tissue.<sup>[1,2]</sup> In healthy young adults, microglia are involved in transient neuroinflammation processes essential for the development and maintenance

M. E. Caetano-Silva, M. T. B. Pacheco  
Center of Food Science and Quality (CCQA)  
Institute of Food Technology (Ital)  
Campinas, SP 13070-178, Brazil

M. E. Caetano-Silva, L. A. Rund, M. Vailati-Riboni, R. W. Johnson  
Department of Animal Sciences  
University of Illinois at Urbana-Champaign  
Urbana, IL 61801, USA  
E-mail: rwjohn@illinois.edu

 The ORCID identification number(s) for the author(s) of this article can be found under <https://doi.org/10.1002/mnfr.202100153>

DOI: 10.1002/mnfr.202100153

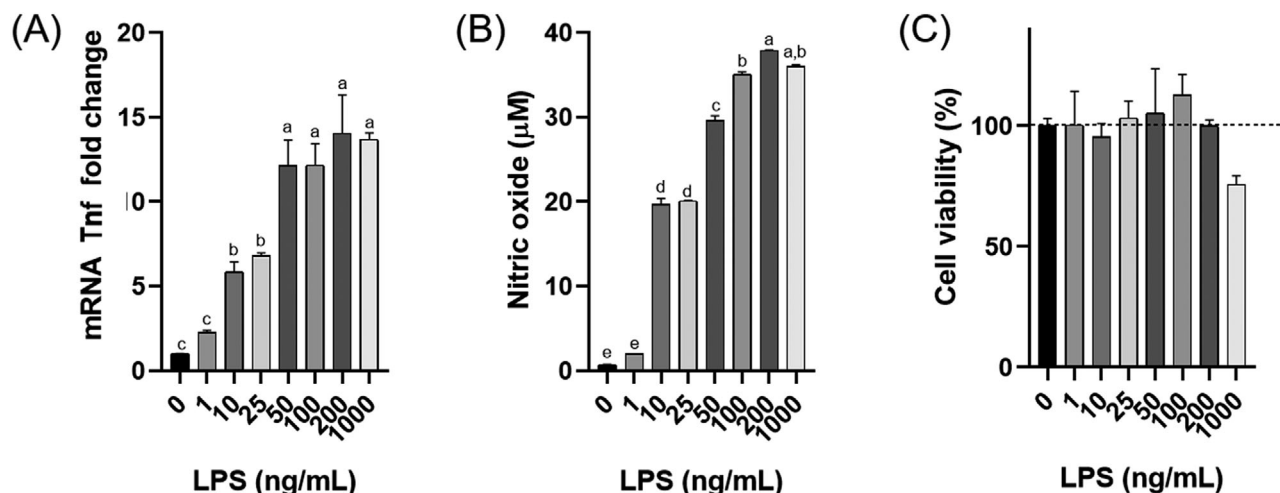


**Figure 1.** LPS dose–response for BV-2 microglial cells. A) mRNA Tnf expression, expressed as fold change in relation to the negative control (cells with no LPS stimulation); B) Nitric oxide; and C) cell viability (% of negative control) measured by MTT assay. Treatments were compared by ANOVA followed by Tukey's test. Different lowercase letters are statistically different ( $p < 0.05$ ) among LPS concentrations.

free radicals by activated microglia can be enhanced due to the excess Fe within these cells.<sup>[18]</sup> The excess of metal ions in central nervous system (CNS) has been reported to be involved in the pathogenesis of neurological diseases related to aging due to their influence on oxidative stress status.<sup>[19]</sup>

In addition, when out of balance, these metal ions can also trigger the aggregation of  $\beta$ -amyloid peptide (A $\beta$ ) and its deposition into amyloid plaques.<sup>[20]</sup> Evidence of the link between AD and redox metal dysregulation has been supported by post-mortem analyses of amyloid plaques, which revealed the accumulation of Cu, Fe, and Zn by 5.7, 2.8, and 3.1 times, respectively, the levels observed in normal brains.<sup>[21]</sup> Chelating compounds might thus prevent the harmful effects of the accumulation of metals. They have been sought as an attractive strategy to alleviate the development and progression of neurological disorders.<sup>[22]</sup>

Considering all these processes, there is an ongoing demand for multifunctional compounds that can act in different ways to hinder the neurodegeneration process through antioxidant, anticholinesterasic, metal-chelating, and anti-inflammatory activities. A number of food-derived peptides have been described as multifunctional compounds, meaning specific sequences within a given peptide can simultaneously exert two or more biological activities.<sup>[23]</sup> Protein derived from a variety of sources, including chia,<sup>[12]</sup> flaxseed,<sup>[24]</sup> soy,<sup>[25]</sup> oyster,<sup>[26]</sup> hazelnut,<sup>[27]</sup> and whey<sup>[28,29]</sup> have been shown to have anti-inflammatory activity. However, the role of specific food-derived peptides and the underlying mechanisms are not fully understood,<sup>[30]</sup> especially in relation to microglia-driven neuroinflammation.

In a previous in vitro study, we demonstrated by biochemical assays that whey peptides with metal-binding capacity present antioxidant and anticholinesterasic activities and, therefore, might represent a source of multifunctional peptides that are neuroprotective.<sup>[31]</sup> In this study, metal-binding peptides from whey protein were further investigated for their ability to inhibit the inflammatory response in activated microglia. The central hypothesis is that peptides with metal-binding capacity can

reduce the expression and secretion of inflammation markers by stimulated microglia.

## 2. Results

### 2.1. Dose-dependent Response of BV-2 Microglia to LPS

LPS stimulation markedly increased both NO and tumor necrosis factor (Tnf) mRNA (Figure 1). Concentrations of 100 and 50 ng mL<sup>-1</sup> elicited a maximal response in NO and Tnf mRNA, respectively, with no impact on cell viability (Figure 1). Based on these findings, a concentration of 50 ng mL<sup>-1</sup> LPS was used in subsequent studies with BV-2 microglia.

### 2.2. Reduction of NO Production

NO concentration in supernatant of unstimulated BV-2 cells ranged between 0 and 0.5  $\mu$ M. LPS stimulation led to high NO production, with supernatant concentration reaching roughly 20  $\mu$ M. Importantly, pretreatment of BV-2 microglia with tH inhibited LPS-induced NO production 16–20% (Figure 2A). The whey hydrophobic peptides (hH) led to a reduction in NO production of 20–58%, suggesting a potential role of the hydrophobic residues in NO release. However, whey metal-binding peptides, when isolated, showed even higher inhibitory effect on the production of NO: the metal-binding peptide treatments resulted in NO production 35–45% lower than the control at 100  $\mu$ g mL<sup>-1</sup>, and 68–76% lower at 1000  $\mu$ g mL<sup>-1</sup>. When comparing to the tH, these values were 22–34% and 60–70%.

### 2.3. Down-regulation of Tnf Gene and TNF- $\alpha$ Protein Expression

LPS stimulation of BV-2 microglia led to a roughly 9-fold increase in Tnf mRNA compared to unstimulated cells, and all whey peptides tested inhibited LPS-induced Tnf mRNA expression.

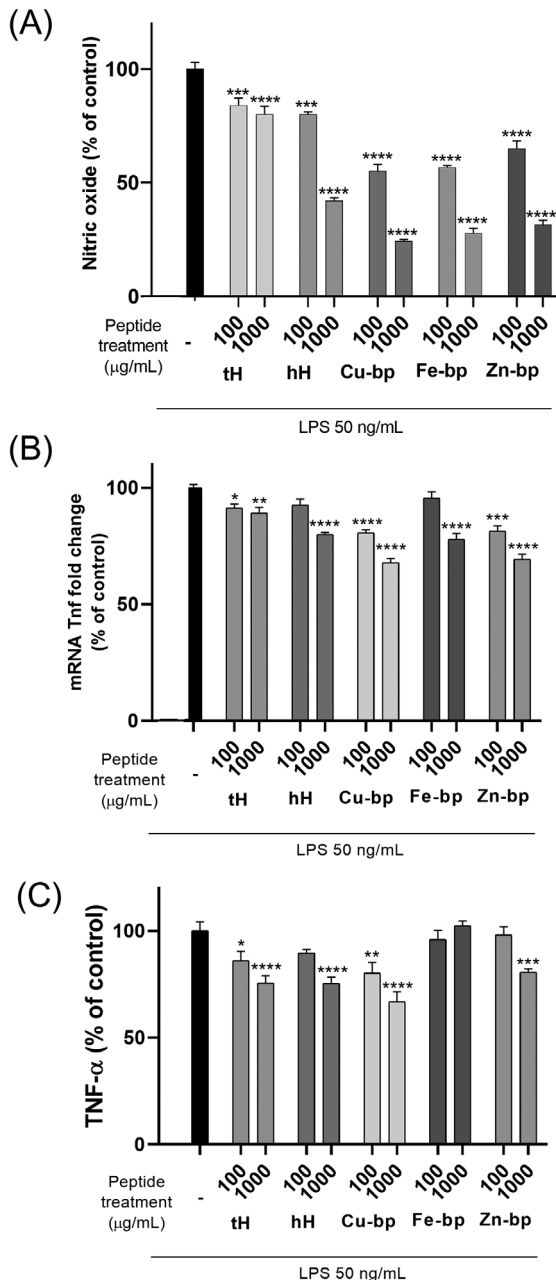


**Figure 2.** Whey metal-binding peptides reduced nitric oxide production and TNF- $\alpha$  expression at mRNA and protein levels in stimulated BV-2 microglial cells. A) Nitric oxide release, B) mRNA Tnf expression, and C) TNF- $\alpha$  release (measured by ELISA) in BV-2 microglial cells expressed as percentage of control (cells stimulated with LPS and no peptide treatment). tH, total whey hydrolysate; hH, hydrophobic fraction of whey hydrolysate; Cu-bp, Fe-bp, and Zn-bp, copper, iron, and zinc-binding peptides from whey hydrolysate, isolated by IMAC. All treatments depicted were stimulated with LPS 50 ng mL<sup>-1</sup>. Negative control assays (cells under all treatments with no LPS stimulation) were carried out, but they did not reach assay sensitivity and are not depicted in the graphs. Samples at 100 and 1000 µg mL<sup>-1</sup> were analyzed by ANOVA followed by Dunnett's test, compared the mean of each sample with the mean of the control (cells stimulated with LPS and no peptide treatment). Statistically different from the control: \*  $p < 0.05$ ; \*\*  $p < 0.01$ ; \*\*\*  $p < 0.001$ ; \*\*\*\*  $p < 0.0001$ . See Supplementary material (Table S1, Supporting Information) for multiple comparisons analysis (ANOVA followed by Tukey's test).

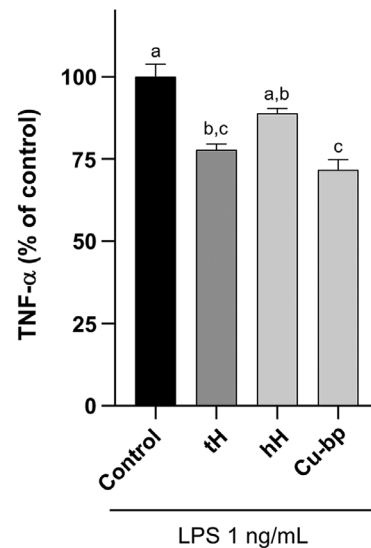


**Figure 3.** Copper-binding peptides reduced TNF- $\alpha$  release by primary microglia from adult mice. TNF- $\alpha$  released (measured by ELISA) by primary microglial cells expressed as percentage of control (cells stimulated with 1 ng mL<sup>-1</sup> LPS and no peptide treatment). tH, total whey hydrolysate; hH, hydrophobic fraction of whey hydrolysate; Cu-bp, copper-binding peptides from whey hydrolysate, isolated by IMAC. All cells were stimulated with LPS 1 ng mL<sup>-1</sup>. Negative control assays (cells under all treatments with no LPS stimulation) were carried out, but they are not depicted in the graphs. Peptide treatment was carried out at 100 µg mL<sup>-1</sup> for 1 h before LPS stimulation. Samples were analyzed by ANOVA followed by Tukey's test for multiple comparisons between each treatment. Different letters are statistically different ( $p < 0.05$ ).

At the highest concentration (1000 µg mL<sup>-1</sup>), tH, hH, and the Cu-bp, Fe-bp, and Zn-bp fractions reduced Tnf mRNA 11–32% (Figure 2B). At the lower concentration (100 µg mL<sup>-1</sup>), tH, hH, and Fe-bp showed no statistical difference with the control, while Zn-bp and Cu-bp reduced Tnf mRNA expression by roughly 20%. These findings were mostly supported by TNF- $\alpha$  protein measured in conditioned supernatants (Figure 2C). Among the metal-binding peptides, only the Cu-bp reduced TNF- $\alpha$  at the lower concentration (100 µg mL<sup>-1</sup>). Interestingly, whereas the Fe-bp reduced Tnf mRNA in BV-2 microglia, it had no effect on the release of TNF- $\alpha$  protein. Collectively, the results suggest that the Cu-bp fraction effects are the most consistent at interfering with LPS-signaling pathways that result in both NO production and TNF- $\alpha$  synthesis and release in BV-2 microglia.

#### 2.4. Reduction of TNF- $\alpha$ Release by Primary Murine Microglia

To verify the Cu-bp fraction would impart anti-inflammatory effects beyond the transfected BV-2 cell line, primary murine microglia were studied. Preliminary studies with 1 ng mL<sup>-1</sup> LPS stimulation elicited the release of TNF- $\alpha$  by roughly 1000 pg mL<sup>-1</sup>. Nitric oxide was also measured in supernatants but was not released even after stimulation with higher LPS concentrations. Cu-binding peptides reduced TNF- $\alpha$  release after LPS stimulation in primary cultures by roughly 30%, while tH reduced release by 22% (Figure 3). Cells pretreated with hH showed no statistical difference in the release of TNF- $\alpha$  compared to the control.

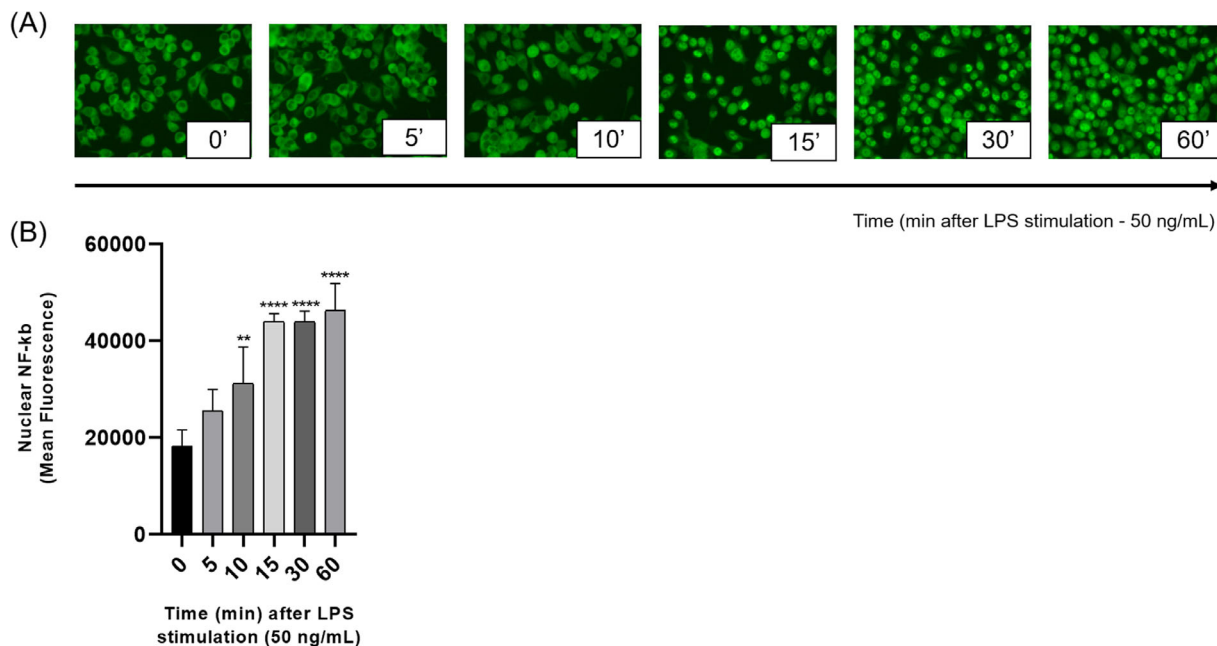


**Figure 4.** A) Fluorescence microscopy depicting immunocytochemical localization of NF- $\kappa$ B p65 (green) and B) nuclear NF- $\kappa$ B p65 (mean fluorescence) of BV-2 microglial cells after different times of 50 ng mL<sup>-1</sup> LPS stimulation (0–60 min). Values were expressed as mean of three independent cellular replicates, whose means resulted from 50 cells from three independent fields of view. Treatments were compared by ANOVA followed by Dunnett's test. Statistically different from the control: \*  $p < 0.05$ ; \*\*  $p < 0.01$ ; \*\*\*  $p < 0.001$ ; \*\*\*\*  $p < 0.0001$ .

Treatments did not affect viability of primary microglia (Figure S2, Supporting Information).

As primary microglia presented the same behavior of BV-2 microglia regarding the effect of Cu-bp treatment on TNF- $\alpha$ , the study of nuclear factor kappa B (NF- $\kappa$ B) translocation was carried out in BV-2 cells.

### 2.5. Suppression of NF- $\kappa$ B p65 Nuclear Translocation in Microglial Cells

In order to explore the underlying molecular mechanisms responsible for inhibition of LPS-induced inflammation, the effect of whey peptides on LPS-induced nuclear translocation of NF- $\kappa$ B p65 was studied using immunofluorescence. Maximal translocation of NF- $\kappa$ B p65 into the nucleus was observed within 15–30 min of LPS stimulation (Figure 4). Therefore, the effects of whey peptides on NF- $\kappa$ B translocation were measured 30 min after LPS stimulation.

Total hydrolysate (tH), its hydrophobic counterpart (hH), and Zn-bp reduced the nuclear translocation of NF- $\kappa$ B p65 in LPS-stimulated BV-2 cells (roughly 16–20%), but to a lower extent than Cu-bp (30% reduction) (Figure 5B). These results are in agreement with our previous results for NO release and Tnf mRNA expression and TNF- $\alpha$  protein release, especially the consistency of Cu-bp effects in all analyses. The effect of fraction Cu-bp on the NF- $\kappa$ B pathway was further corroborated in primary microglia wherein Cu-bp reduced ( $p < 0.05$ ) the LPS-induced nuclear translocation of the subunit NF- $\kappa$ B p65 (Figure 5C). These results suggest that the inhibitory effects of whey peptides are at least partially due to inhibition of the of NF- $\kappa$ B pathway.

### 2.6. Potential Bind of NF- $\kappa$ B p65 and Metal-binding Peptides: Molecular Docking Studies

The minimum estimated free energies (EFE) (kcal mol<sup>-1</sup>) indicate the level of possible interactions between receptor and ligand, i.e., the binding affinity (Table 1). The more negative the value, the more likely the ligand is to inhibit the receptor. The Cu-bp presented a number of peptides with higher affinity for NF- $\kappa$ B p65 than the Fe-bp fraction. The highest affinity was observed for the peptide FNPT (-8.8), also identified on Zn-bp fraction. This absolute value is higher than the observed for chia peptides potential interaction with NF- $\kappa$ B p65 reported by Grancieri et al.<sup>[32]</sup> Table 2 presents the chemical interactions among some of the Cu-binding peptides with the NF- $\kappa$ B p65, and Figure 6 depicts the 2D diagrams of such interactions. The EFE for JSH23 was -5.9, and it possibly interacts with the receptor at three different sites, by van der Waals, hydrogen bond, and alkyl interactions (Table 2). In the meantime, 15 out of 17 sequences identified on Cu-bp presented better affinity values than the pharmacological control (-6.0 to -8.8.) (Table 1), and multiple possible sites of interaction (Table 2 and Figure 6).

### 3. Discussion

To our knowledge, this is the first study to investigate if whey metal-binding peptides inhibit inflammation pathways in microglia. Previous work on the potential neuroprotective activity of metal-binding peptides demonstrated that Cu-binding peptides have in vitro antioxidant and anticholinesterasic activities.<sup>[31]</sup> In the present work, these peptides were further studied in microglia the resident immune cell in the CNS that respond to and



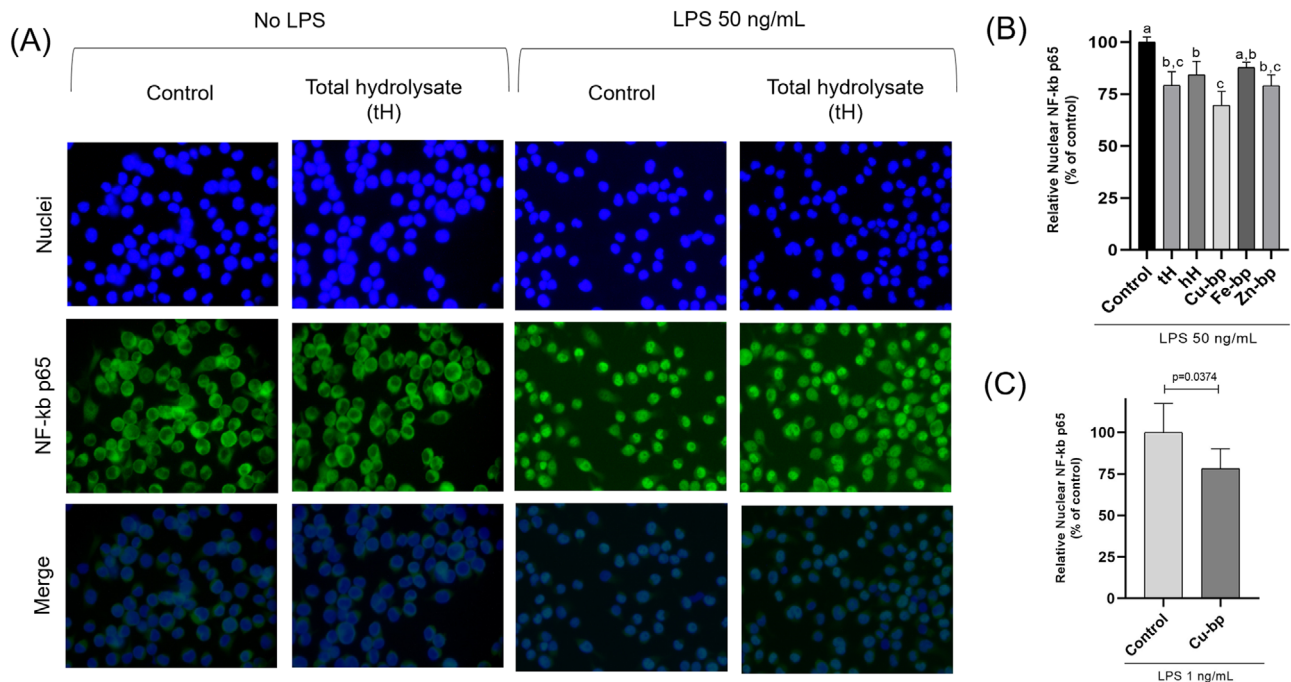


**Figure 5.** Pretreatment with whey metal-binding peptides affected nuclear translocation of NF-κB p65 in microglial BV-2 cells and primary microglia from adult mice 30 min after stimulation with LPS. **Panel A.** Fluorescence microscopy depicting immunocytochemical localization of NF-κB p65 (green) and nuclei staining (blue) of control (no peptide treatment) and total hydrolysate (tH) treatment ( $100 \mu\text{g mL}^{-1}$ ) with no stimulation (six pictures on the left) and LPS  $50 \text{ ng mL}^{-1}$  stimulation (six pictures on the right) in microglial (BV-2) cells. **Panels B and C.** Relative Nuclear NF-κB of BV-2 cells and primary microglia, respectively, expressed as percentage of control (cells stimulated with LPS and no peptide treatment). tH, total whey hydrolysate; hH, hydrophobic fraction of whey hydrolysate; Cu-bp, Fe-bp, and Zn-bp, Copper, Iron, and Zinc-binding peptides from whey hydrolysate, isolated by IMAC. Peptide treatment was carried out at  $100 \mu\text{g mL}^{-1}$  for 1 h before LPS stimulation. Negative control assays (cells under all treatments with no LPS stimulation) were carried out, but they are not depicted in the graph. Values were expressed as mean of at least three independent replicates, whose means resulted from 50 cells from three independent fields of view. Treatments were compared (B) by ANOVA followed by Tukey's test for multiple comparisons between each treatment; different letters are statistically different ( $p < 0.05$ ); or (C) by  $t$  test comparing control and treatment with Cu-bp in primary microglia.

**Table 1.** Identified peptides in metal-binding fractions and their estimated free energy binding (EFE) ( $\text{kcal mol}^{-1}$ ) to NF-κB p65.

Cu-bp		Fe-bp		Zn-bp		Pharmacological control	
Peptide	EFE [ $\text{kcal mol}^{-1}$ ]	Peptide	EFE [ $\text{kcal mol}^{-1}$ ]	Peptide	EFE [ $\text{kcal mol}^{-1}$ ]		EFE [ $\text{kcal mol}^{-1}$ ]
FNPT	-8.8	DISLL	-6.7	FNPT	-8.8	JSH3	-5.9
SAPLRVY	-8.3	LIVTQ	-6.6	HLLR	-7.6		
PLRVY	-8.1	LSFNPT	-6.2	KIPAVF	-7.2		
ALKALPM	-7.3	SDISLL	-5.8	ALPM	-6.8		
KIPAVF	-7.2	LLR	-5.7	LIVTQ	-6.6		
KIPAVFK	-7.0	VEELKPTPEGDLEIL	-5.1	KTKIPAV	-6.6		
KVLVL	-6.8			TKIPAVF	-6.5		
ALPM	-6.8			LLR	-6.4		
LIVTQ	-6.8			KTKIPAVF	-6.1		
KILDKVGIN	-6.7			KALPM	-6.0		
LKALPM	-6.6			VF	-5.4		
TKIPAVF	-6.5						
DKALKALPM	-6.4						
KTKIPAVF	-6.1						
KALPM	-6.0						
KIL	-5.4						
PM	-4.6						

EFE - minimum estimated free energies; indicate the level of possible interactions between receptor and ligand.

**Table 2.** Estimated free energy binding (EFE) (kcal mol<sup>-1</sup>) and chemical interactions among the whey metal-binding peptides with the DNA-binding site of NF-kB p65.

Peptide	EFE [kcal mol <sup>-1</sup> ] <sup>a)</sup>	Interacting amino acid residues <sup>b)</sup>	Type of interaction
FNPT	-8.8	THR D:239, ARG D:242, MET D:271, GLY D:273, GLY D:274, THR D:276, GLY D:279, LEU D:283, GLU D:302, ASP D:303, GLY D:304, GLY D:279, GLU C:211, PHE C:213, ASP C:243	van der Waals
		ARG D:275, HIS C:245, ALA C:242, ARG C:246	Conventional hydrogen bonds
		PRO D:301, CYS D:240, VAL C:251	Pi-Alkyl
KIPAVF	-7.2	PRO D:301, ASP D:303, MET D:271, GLY D:273, GLY D:274, THR D:276, GLU C:222, ALA C:242, VAL C:244, HIS C:245, GLN C:247	van der Waals
		ARG D:275, LYS C:221, GLN C:241, ARG C:246	Conventional hydrogen bonds
		GLY D:304	Carbon hydrogen bonds
KVLVL	-6.8	LEU D:282, LEU D:283	Pi-Alkyl
		ARG D:242, CYS D:240, GLU D:250, MET D:271, GLY D:273, GLY D:274, THR D:276, PRO D:301, GLU D:302, ASP D:303, VAL C:244, ARG C:246, VAL C:251	van der Waals
		ARG D:275, ASP C:243	Conventional hydrogen bonds
Pharmacological control (JSH23)	-5.9	GLY D:274	van der Waals
		ARG D:275	Conventional hydrogen bonds
		LEU D:283	Pi-Alkyl

<sup>a)</sup> EFE - minimum estimated free energies; indicate the level of possible interactions between receptor and ligand; <sup>b)</sup> Each interacting amino acid residue is represented by the 3 letters code; a letter (D or C) related to the NF-kB p65 chain, and a number, related to its position in the NF-kB p65 sequence.

propagate inflammatory signals initiated at the periphery.<sup>[1,2]</sup> Activation of microglia via immune signaling pathways culminates in the release of inflammatory mediators, such as NO, oxygen radicals, and pro-inflammatory cytokines.<sup>[33]</sup> Neuroinflammation driven by microglia is closely related to the etiology and progression of neurodegenerative diseases including Alzheimer's disease, Parkinson's disease, and multiple sclerosis.<sup>[9]</sup> Consequently, microglia have become an important treatment target for numerous neuropsychiatric and neurodegenerative diseases.<sup>[10]</sup> Thus, finding compounds that can regulate microglia function in the brain to decrease neurotoxic inflammatory mediators is of utmost importance.

Whey peptides reduced inflammation markers in microglia (NO and TNF- $\alpha$ ) after LPS-stimulation, and Cu-binding peptides fraction showed anti-inflammatory effects in both BV-2 (Figure 2) and primary (Figure 3) microglia. Excessive NO production by microglial cells has been identified as a contributing factor in the pathogenesis of neurodegenerative diseases,<sup>[13]</sup> while TNF- $\alpha$  is one of the major inflammatory mediators.<sup>[28]</sup>

The Cu-bp consists of highly hydrophobic peptides, with the ability to bind copper. The presence of the hydrophobic amino acids might facilitate the solubility of the peptides in lipids, enhancing the interaction between peptide and receptors on the surface of cells, which may contribute toward modulating the downstream signaling pathways and exhibiting the anti-inflammatory effect.<sup>[34]</sup> Peptides with hydrophobicity up to 20 kcal mol<sup>-1</sup> tend to be more effective for penetrating the cell membrane, and thus present the inhibitory effect by binding specific molecules.<sup>[35]</sup> All the peptides found in the Cu-bp fraction have hydrophobicity val-

ues between 6.1 and 15.2 kcal mol<sup>-1</sup>. Besides the hydrophobicity, some specific amino acid sequences of peptides with Cu-binding capacity can also play a crucial role. The whole hydrolysate (tH) and its hydrophobic counterpart (hH) showed no difference on TNF- $\alpha$  release and NF-kB nuclear translocation, although hH was more efficient in reducing the NO release. A different behavior for both markers was also observed for the Fe-bp fraction, suggesting that the process to obtain hH has possibly concentrated hydrophobic peptides with no effect (e.g., peptides present on Fe-bp, which presented no activity in reducing TNF- $\alpha$  release—Figure 2C, and suppressing NF-kB p65 nuclear translocation—Figure 5B), resulting in lower activity comparing to both Cu-bp and tH, at least in the NF-kB pathway.

Most of the studies on anti-inflammatory food-derived peptides have been carried out first using transformed cell lines.<sup>[36]</sup> In the present study, the microglia cell line BV-2 was successfully used as a screening tool to assess the anti-inflammatory activity of peptides and the understanding of possible mechanisms involved in this activity, e.g., the NF-kB pathway. Subsequently, due to the number of microglia that can be isolated from the mouse brain, a limited set of studies was done with primary murine microglia to corroborate the activity of Cu-binding peptides in inhibiting the TNF- $\alpha$  production (Figure 3) and the nuclear translocation of the subunit NF-kB p65 (Figure 5C). This is important because primary microglia retain their in vivo phenotype.<sup>[37]</sup> In vivo studies on the effects of whey peptides on neuroinflammation will be a logical next step, but cannot be completed now due to the limited availability of the purified peptides.

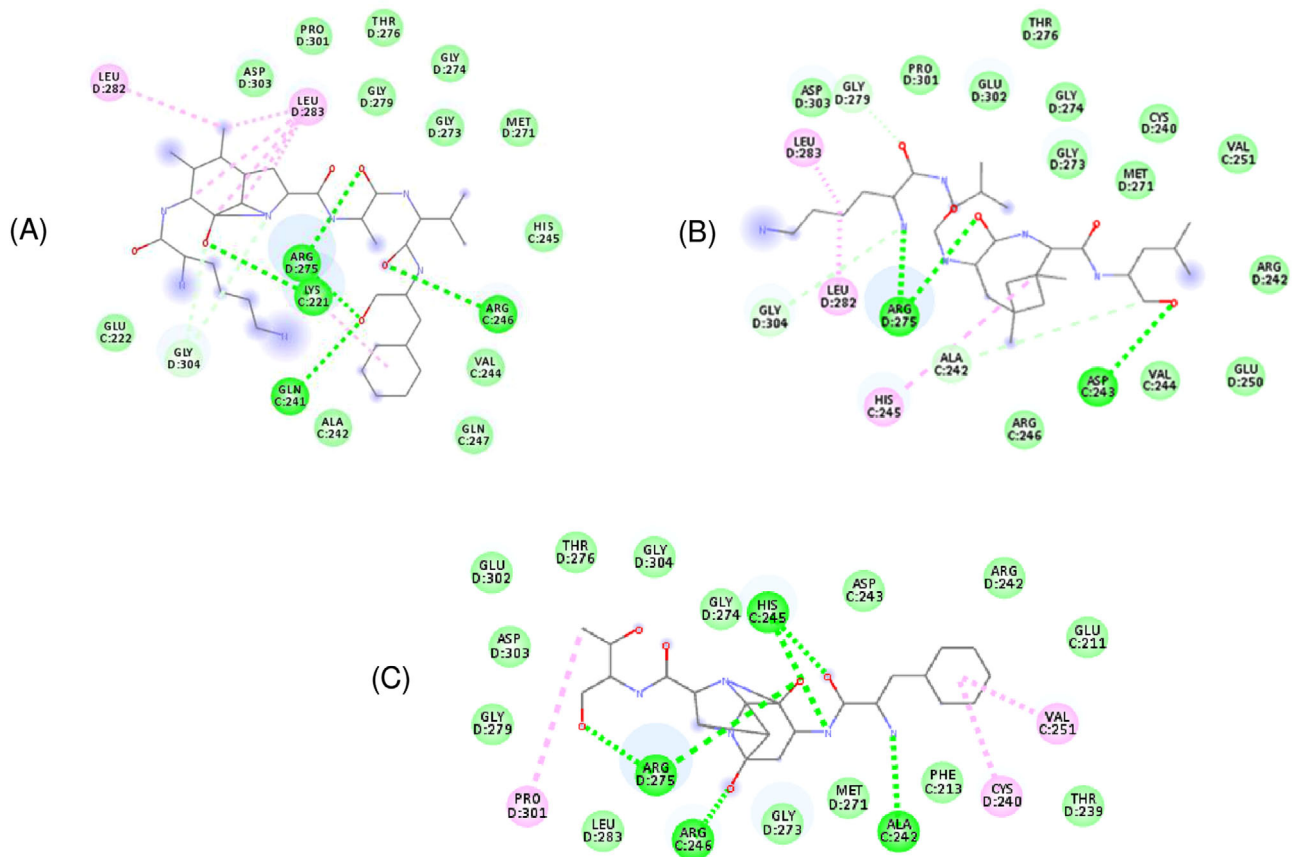


**Figure 6.** Molecular docking 2D diagrams exemplifying the interaction of amino acid residues from receptor NF- $\kappa$ B p65 and some whey Cu-binding peptides: A) KIPAVF (Lys-Ile-Pro-Ala-Val-Phe); B) KVLVL (Lys-Val-Leu-Val-Leu); C) FNPT (Phe-Asn-Pro-Thr). The colorful pallets represent different interacting amino acids residues of NF- $\kappa$ B p65, and different colors represent different interaction type. Each interacting amino acid residue inside the pallet is represented by the three letters code; a letter (D or C) related to the NF- $\kappa$ B p65 chain, and a number, related to its position in the NF- $\kappa$ B p65 sequence. The metal-binding peptides are represented in black lines primary structures. The oxygen and nitrogen atoms are highlighted in red and blue, respectively.

Among the pro-inflammatory factors secreted by activated microglia, oxygen and nitrogen reactive species, including NO and superoxide, can contribute to the oxidative stress in the environment. The inflammatory process is closely related to oxidative stress since inflammation and reactive oxygen species (ROS) stimulate each other, causing a vicious cycle.<sup>[12]</sup> Oxidative stress has been associated with chronic inflammation in several neurodegenerative diseases.<sup>[11]</sup> The antioxidant property of some anti-inflammatory peptides may further contribute to their anti-inflammatory effects.<sup>[30]</sup> NF- $\kappa$ B is a redox-sensitive transcription factor, and is closely associated with oxidative stress. Moreover, suppression of NF- $\kappa$ B has been shown to improve antioxidant defense.<sup>[38]</sup> In a previous study, Cu-bp showed higher in vitro antioxidant activity than Fe-bp,<sup>[31]</sup> which can be somehow related to the anti-inflammatory activity observed in microglia in this study. Further studies on oxidative stress are needed to clarify the relation between antioxidant and anti-inflammatory activities.

NF- $\kappa$ B plays a central role as an inducible transcription factor and is critical for the regulation of inflammatory genes.<sup>[28]</sup> In unstimulated cells, the NF- $\kappa$ B is located in the cytoplasm, in an inactive form, bond to inhibitor  $\kappa$ B (I $\kappa$ B) proteins. Inflammatory stimuli lead to phosphorylation of the I $\kappa$ B (the inhibitor

of NF- $\kappa$ B) molecules resulting in the degradation of I $\kappa$ B. Therefore, NF- $\kappa$ B subunits, p50 and p65, become free to migrate into the nucleus and activate the transcription of various genes involved in inflammation.<sup>[34]</sup> The predominant activated form of NF- $\kappa$ B in mature glial cells is reported to contain the p65 subunit, rather than utilizing non-canonical signaling mediated by other heterodimers.<sup>[39]</sup> The immunofluorescence studies clearly showed that specifically this p65 subunit was in the cytosol and, upon stimulation, it went to the nucleus (Figure 4). When pre-treated with whey peptides, specially Cu-bp, the migration of this subunit to the nucleus was significantly decreased (Figure 5).

Mechanistically, the results showed that whey metal-binding peptides could alleviate the inflammatory response in microglia by suppressing the translocation of NF- $\kappa$ B p65 to the nucleus. Cu-bp showed potential to inhibit this process both in transformed cell line BV-2 and primary culture (Figure 5). NF- $\kappa$ B inhibitors can either inhibit the activation/phosphorylation of I $\kappa$ B and its degradation, thus preventing the release of free NF- $\kappa$ B, or interfere directly with the DNA-binding region in the NF- $\kappa$ B.<sup>[40]</sup> Although the exact mechanisms by which whey peptides suppress NF- $\kappa$ B nuclear translocation are unclear, the molecular docking calculations corroborated the possibility of acting by

direct interaction to the NF- $\kappa$ B p65 subunit. Most of the peptides identified on Cu-bp (15 out of 17) showed affinity values higher than the pharmacological control JSH3. Fe-bp fraction, instead, presented peptides with a lower affinity toward NF- $\kappa$ B p65 than the ones in Cu-bp (Table 1), which might be related to the lower ability of Fe-bp to suppress NF- $\kappa$ B nuclear translocation (Figure 5). Thus, the binding affinity assessed computationally aligns with what was observed in the immunofluorescence experiment.

The potential interactions between the amino acid residues of the receptor (NF- $\kappa$ B p65) and the amino acid residues of the ligands (whey peptides) comprise van der Waals, hydrogen bonds, and alkyl interactions. The multiple possible sites of interaction suggest that the Cu-bp could form a strong network of interactions with NF- $\kappa$ B p65. The number of possible hydrogen bonds could increase the strength of such a network since this type of interaction is related to binding strength and indispensable for the stability of a protein and its complex.<sup>[41]</sup> Moreover, strong hydrogen bonds may mask important amino acids in the NF- $\kappa$ B chain and also influence the conformation of p65 required for DNA binding.<sup>[40]</sup> Also, the majority of interactions with amino acid residues from NF- $\kappa$ B occur through van der Waals interactions (Table 2), which means the hydrophobicity plays a crucial role in the binding affinity among whey peptides and NF- $\kappa$ B. The hydrophobicity of peptides from Cu-bp ranged from 6.1 to 15.2 kcal mol<sup>-1</sup>, while the peptides from Fe-bp fraction showed values as high as 25.21 kcal mol<sup>-1</sup>.<sup>[31]</sup> This might be a factor that decreases the ability of the peptides from this fraction to both penetrate the cell membrane and bind with NF- $\kappa$ B.

The difference in the peptide structures can also influence the ability of such peptides to bind to other protein molecules such as NF- $\kappa$ B. For instance, Lys is a positively charged residue and is more likely to approach anionic binding sites. The percentage of Lys in Cu-bp is 4-fold higher than in the fragments from Fe-bp.<sup>[31]</sup>

Apart from the NF- $\kappa$ B pathway, other mechanisms can be involved since different intracellular signaling pathways, including mitogen-activated protein (MAP) kinases and activator protein-1 (AP-1) can be activated, leading to inflammation.<sup>[36]</sup> Fe-bp presented the capacity to decrease NO release (Figure 2), but did not affect the translocation of NF- $\kappa$ B into the nucleus (Figure 5). Therefore, these specific peptides might act through a different mechanism, such as AP-1. For example, on the one hand, Grancieri et al.,<sup>[12]</sup> studying different anti-inflammatory peptide fractions from chia protein, observed that the most potent fraction to decrease NO release in stimulated macrophages was the same with the highest activity in decreasing AP-1 expression. On the other hand, although this fraction was also able to decrease TNF- $\alpha$  release and nuclear translocation of NF- $\kappa$ B p65, there was no difference compared to other fractions, suggesting that the release of TNF- $\alpha$  and NO might be triggered by distinct pathways. Even though NF- $\kappa$ B and AP-1 transcription factors are regulated by different mechanisms, they appear to be activated simultaneously by the same multitude of stimuli.<sup>[42]</sup> Specifically, LPS stimulation can activate both NF- $\kappa$ B or AP-1<sup>[12,43]</sup>; thus, both might be activated in this study.

There has been a broad search for multitargeted compounds in recent years due to the different mechanisms associated with the neurodegenerative processes. This study brings a new approach of using food-derived peptides for neuroprotective purposes, in-

cluding the isolation of the ones with metal-binding capacity. The approach of using food-derived peptides as multifunctional compounds has the advantage of multiple compounds that can present beneficial effects through different mechanisms at the same time, since there are different structures within the fractions studied.

The present study corroborates the possibility of using food-derived peptides to reduce inflammation, which may be neuroprotective. Nevertheless, microglia are multifunctional cells that interact with numerous other cells in the CNS, including neurons, astrocytes, and oligodendrocytes.<sup>[10]</sup> Understanding the complexity of several pathways on the CNS, such as NF- $\kappa$ B, is even harder specifically due to the vast cell-type heterogeneity in this system and the interplay between them.<sup>[39]</sup> Thus, we acknowledge that these peptides could also act in other cells beyond microglia and there are still crucial mechanisms that need to be fully elucidated. An open question is whether peptides derived from consuming dairy products reach a sufficient concentration to affect brain microglia. Treatment of CD11b-positive primary microglia with peptides derived from dairy products ranging from 62.5 to 250  $\mu$ g mL<sup>-1</sup> have been reported to suppress TNF- $\alpha$  production in LPS-stimulated cells.<sup>[44]</sup> In other studies, these same peptides have been shown to penetrate the blood-brain barrier (BBB)<sup>[45]</sup> and to reduce the levels of inflammatory cytokines, suppress the number of activated microglia in cerebral cortical tissue, and ameliorate impaired long-term object memory in an Alzheimer mouse model.<sup>[46]</sup> We acknowledge that each peptide can behave differently and the peptides need to be further studied in an in vivo model to determine the efficacy of the whey Cu-binding peptides as anti-inflammatory compounds on microglial cells in vivo. However, the present study is a necessary first step towards understanding how these peptides can act as anti-neuroinflammatory compounds. The present results, coupled with the previously reported ones,<sup>[31]</sup> suggest that the Cu-binding peptides might represent food-derived peptides with potential to be neuroprotective.

## 4. Conclusion

Cu-binding peptides presented anti-inflammatory activity by down-regulating inflammatory markers in both BV-2 and primary microglia. The inhibitory effect seems to occur by suppressing the NF- $\kappa$ B pathway, potentially by direct interaction of specific peptide sequences with the binding site of NF- $\kappa$ B p65. It is worthy to highlight that microglia interact with other cells in the CNS, thus future studies are needed to assess the efficacy of those peptides in inhibiting neuroinflammation in vivo. The chelation of excess copper by these peptides, as well as their bioavailability and their capacity to cross the BBB, are also crucial factors that can contribute to their future application.

## 5. Experimental Section

**Material:** Whey protein isolate (WPI) Provon 292 was obtained from Glanbia Nutritionals (Kilkenny, Ireland). The alkaline protease (Alcalase) was purchased from Davisco Foods International, Inc. (Le Sueur, MN, USA). The CuSO<sub>4</sub>·5H<sub>2</sub>O and FeCl<sub>3</sub>·6H<sub>2</sub>O and the LPS (*Escherichia coli* 0127:B8) were purchased from Sigma-Aldrich (St. Louis, MO, USA). The ZnSO<sub>4</sub>·7H<sub>2</sub>O was purchased from Scharlab (P. I. Mas d'en Cisa,



Barcelona, Spain). All other chemicals and reagents were of analytical or chromatographic grade.

**Whey Protein Hydrolysate and Metal-binding Fractions Obtention:** The peptide fractions with affinity to Cu, Fe, and Zn were obtained according to previously described.<sup>[31]</sup> Briefly, whey protein isolate was resuspended in deionized water (7% w/v) and hydrolyzed with alkaline protease (Alcalase) (enzyme: substrate ratio 1:100 w/w) under pH 8.5 and 60 °C with constant stirring during 180 min. The enzyme was deactivated by heating (90 °C for 10 min). The hydrolysate was immediately cooled and then freeze-dried. The hydrolysate was named total hydrolysate (tH) (degree of hydrolysis—according to Adler-Nissen<sup>[47]</sup>—20.89%) and used as a control in all the experiments.

The hydrolysate was subjected to isolation of metal-binding peptides by Immobilized Metal Affinity Chromatography (IMAC). Iminodiacetic Acid Sepharose (I4510, Sigma-Aldrich) was loaded with  $\text{CuSO}_4 \cdot 5\text{H}_2\text{O}$ ,  $\text{ZnSO}_4 \cdot 7\text{H}_2\text{O}$ , or  $\text{FeCl}_3 \cdot 6\text{H}_2\text{O}$  and the metal-binding peptides were isolated as previously described.<sup>[31]</sup> The binding-peptides were treated with Chelex resin (Chelex-100, Sigma-Aldrich, St. Louis, MO, USA) (1:2 m/v;  $25 \pm 2$  °C  $2 \text{ h}^{-1}$  under stirring) to remove any possible trace of metal ions. The binding-peptides were further purified by SPE using Oasis HLB (hydrophilic-lipophilic balance) cartridge 200 mg, 30  $\mu\text{m}$  (Waters Corporation, Milford, MA, USA). The purified fractions were named “[metal]-bp” standing for binding peptides. All the fractions were metal free and contain only metal-binding peptides. The tH was also subjected to purification by HLB cartridge, thus obtaining only the hydrophobic peptides (hH).

**BV-2 Microglia LPS Stimulation and Treatment with Metal-binding Peptides:** The BV-2 murine microglia cell line was obtained from the American Type Culture Collection, and all assays were performed between passages 19 and 28. The cells were cultured in 75  $\text{cm}^2$  tissue culture flasks (BD Falcon) in DMEM supplemented with 4 mM L-glutamine, 1mM sodium pyruvate, 10% fetal bovine serum (FBS), 1% Penicillin–Streptomycin (10000 U  $\text{mL}^{-1}$ ), and maintained at 37 °C in a humidified incubator under 5%  $\text{CO}_2$ . When cells reached confluence, they were gently detached using a cell scraper and centrifuged (1000  $\times$  g/5 min). The cells were resuspended in 2% FBS DMEM and seeded in 96-well plates ( $3.1 \times 10^4$  cells per well).

A preliminary study was done to identify a concentration of LPS that elicited an intermediate inflammatory reaction and that was not toxic. LPS was dissolved in 2% FBS DMEM and cells were incubated with 0, 1, 10, 25, 50, 100, 200, and 1000  $\text{ng mL}^{-1}$  LPS for 24 h in three independent replicates. TNF- $\alpha$  and NO were measured in supernatants as described below and cell viability was assessed using the MTT ((3-(4,5-Dimethylthiazol-2-yl)-2,5-Diphenyltetrazolium Bromide) assay in accordance with the manufacturer's instructions (Thermo Fisher Scientific, Waltham, MA, USA, cat M6494). The optimal concentration was determined to be 50  $\text{ng mL}^{-1}$  and was used for subsequent experiments with BV-2 cells.

To assess effects of whey peptides, BV-2 cells were treated with peptides (0, 100, or 1000  $\mu\text{g mL}^{-1}$ ) for 1 h and then stimulated with LPS (0 or 50  $\text{ng mL}^{-1}$ ) for 24 h. The study was repeated, and each study included three independent treatment replicates. The supernatant was collected and stored at  $-80$  °C for subsequent analysis of NO and TNF- $\alpha$ . The attached cells were then subjected to lysis for RNA isolation. Treatment effects on cell viability were also assessed using the MTT assay.

**Nitric Oxide Production:** NO production was measured by determination of nitrite, a stable reaction product of NO with molecular oxygen, using the Griess method. Briefly, 50  $\mu\text{L}$  of supernatant from each treatment or 50  $\mu\text{L}$  of standard solution was mixed with 50  $\mu\text{L}$  Griess reagent (Cayman Chemical, Ann Arbor, MI, USA) (mixture Griess A and B 1:1). The 96-well plate was then incubated for 10 min at room temperature protected from light. The absorbance values were read at 540 nm. The concentration of NO was measured using a standard curve of  $\text{NaNO}_2$  (1.25–40  $\mu\text{M}$ ).

**Tnf mRNA and TNF- $\alpha$  Protein:** Tnf mRNA was measured by Quantitative real-time PCR (qRT-PCR) and TNF- $\alpha$  protein in supernatants was measured by ELISA.

**qRT-PCR.** After addition of 100  $\mu\text{L}$  of TRK lysis buffer (with 2% 2-mercaptoethanol) to each well, total RNA was isolated from BV-2 cells using the E-Z 96 Total RNA Kit according to the manufacturer's instructions, including on-membrane DNase I Digestion step (Omega Bio-Tek,

Norcross, GA, USA). The RNA was quantified using a Nanodrop spectrophotometer (Thermo Fisher). cDNA was synthesized from 200 ng of RNA using the High-Capacity cDNA Reverse Transcription Kit with RNase Inhibitor kit (Thermo Fisher, cat 4374967) following manufacturer's instructions, with the addition of 5  $\mu\text{M}$  of OligodT18 (Integrated DNA Technologies) per reaction. Quantitative PCR was performed using 4.5  $\mu\text{L}$  of diluted cDNA and 5.5  $\mu\text{L}$  of a mastermix composed of 10 parts of Taq-Man Universal PCR Master Mix (Thermo Fisher, cat 4324020) and 1 part of 20x commercially available pre-made primer assay. FAM was selected for probe, and primer to probe ratio was set at 2:1. Tnf and GAPDH (Glyceraldehyde 3-phosphate dehydrogenase) (Mm.PT.58.29509614 and Mm.PT.39a.1 PrimeTime qPCR Assay, Integrated DNA Technologies) were selected as target gene and internal control, respectively. Reactions were run on a QuantStudio 7 real time PCR machine (Thermo Fisher) using the relative standard curve method (generated from a pool of all cDNA pre-dilution), and following the polymerase manufacturer recommended thermal cycle. Results were analyzed on the QuantStudio Real-Time PCR software and relative quantities were exported. Prior to statistical analysis, target gene relative quantities were normalized using relative quantities of the internal control gene, and log<sub>2</sub> transformed to normalize their distribution.

**ELISA.** The TNF- $\alpha$  concentration of cell supernatants was assessed using a specific ELISA kit (Thermo Fisher, cat 88-7324-88) following the manufacturer's instructions.

**Primary Microglia Isolation:** All studies were carried out in accordance with the United States National Institutes of Health guidelines and approved by the University of Illinois Institutional Animal Care and Use Committee. Male and female C57BL/6J mice (Jackson Laboratories No. 000664) bred in the colony were used for all experiments. They were maintained in a temperature-controlled environment with a 12-h reversed-phase light/dark cycle (lights on 22:00 h) and provided with ad libitum water and Teklad Diet 2918. Mice were euthanized by  $\text{CO}_2$  asphyxiation and then transcardially perfused with sterile ice-cold PBS. The brains were collected and immediately used for microglia isolation using the Neural Tissue Dissociation Kit P (Miltenyi Biotec, Germany), according to Nikodemova and Watters<sup>[48]</sup> with adaptations. The brains of 10 adult mice (10–12 weeks of age; five males and five females) were used for each experiment.

Brains were enzymatically digested in a gentleMACS Octo Dissociator at 37 °C for 22 min. The following steps were performed at 4 °C. Tissue debris was removed by passing the cell suspension through a 70  $\mu\text{m}$  cell strainer in Hank's Balanced Salt Solution (HBSS). After centrifugation, the pellet was resuspended in 30% Percoll Plus (GE Healthcare, Princeton, NJ, USA), and further centrifuged to remove myelin and other cells in the supernatant. The pellet containing microglial cells was treated with 1x RBC removal solution (Miltenyi Biotec) to remove red blood cells, and microglia were labeled with anti-CD11b magnetic beads (Miltenyi Biotec) in PEB buffer (PBS supplemented with 0.5% BSA and 2 mM EDTA) for 22 min at 4 °C. CD11b<sup>+</sup> cells were separated in a magnetic field using MS columns (Miltenyi Biotec). After centrifugation, microglia were resuspended in 10% FBS DMEM at 37 °C, counted using Cell Counter, and immediately plated in a 96-well plate ( $1 \times 10^5$  cells per well; 200  $\mu\text{L}$  per well). The cells were allowed to attach during an overnight incubation at 37 °C in a humidified incubator under 5%  $\text{CO}_2$ . Then, the culture medium was changed to fresh culture medium containing the whey peptides (0 or 100  $\mu\text{g mL}^{-1}$ ). After 1 h treatment, cells were stimulated with LPS (0 or 1  $\text{ng mL}^{-1}$ ) for 24 h. A lower concentration of LPS was used because primary microglia are significantly more sensitive than BV-2 cells. The viability of microglial cells was evaluated using the MTT assay.

**Nuclear Translocation of NF- $\kappa\text{B}$  p65:** To determine the optimum time to measure nuclear translocation, a time-response assay for LPS stimulation was carried out without the peptides. Measurements were made at points from 0 to 60 min as the nuclear translocation of NF- $\kappa\text{B}$  occurs within 60 min after stimulation.<sup>[49]</sup> The cells were cultured as described above (item “BV-2 Microglia LPS Stimulation and Treatment with Metal-binding Peptides”) and then treated with peptides for 1 h prior to LPS stimulation (50  $\text{ng mL}^{-1}$ ). At the 30 min optimum time point, the BV-2 cells were washed with PBS and fixed with 4% PFA for 10 min. The PFA

was removed and the cells were washed with PBS 3 times and blocked (5% goat serum in 1x PBS 0.3% Tween) for 1 h.

The primary antibody NF- $\kappa$ B p65 (D14E12) XP Rabbit mAb (Cell Signaling Technology, Inc., Danvers, MA, USA) was diluted (1:400) in antibody dilution buffer (1X PBS / 1% BSA / 0.3% Triton X-100) and incubated overnight at 4 °C. The cells were stained with the secondary antibody [Alexa Fluor 488 Goat anti-Rabbit IgG (H+L) - dilution 1:1000 in antibody dilution buffer] for 1 h protected from light. Cells were then incubated with Hoechst (Life Technologies, Cat H3570, 10 mg mL<sup>-1</sup>, Eugene, OR, USA) for 5 min protected from light.

The images were acquired using a Laxco LMI 6-FL88 inverted microscope with epifluorescence, a 40X (NA 0.65) objective, and 5.1MP CMOS camera. The nuclear translocation of NF- $\kappa$ B p65 was analyzed by determining the fluorescence intensity in the nucleus of the stained cells, using the ImageJ software (U. S. National Institutes of Health, Bethesda, MD, USA, <https://imagej.nih.gov/ij/>, 1997–2018). These intensity values are reported as the percentage of level measured in control (cells not treated with peptides but stimulated with LPS 50 ng mL<sup>-1</sup>), which was considered 100%.

The nuclear translocation of NF- $\kappa$ B p65 was also evaluated in primary microglia treated with the selected sample Cu-bp. The cells were cultured as described above (item “Primary microglia isolation”) and then treated with Cu-bp (100  $\mu$ g mL<sup>-1</sup>) for 1 h prior to 30 min LPS stimulation (1 ng mL<sup>-1</sup>). Immunofluorescence staining was carried out as above described.

**Sequencing and Molecular Docking:** The metal-binding peptides from IMAC fractions were previously sequenced by high-resolution mass spectrometry (HRMS).<sup>[31]</sup> The software PepSeq MFC Application 3.4.0.1 was used to sequence the peptides manually.

The possible interactions of the previously identified peptides<sup>[31]</sup> with the NF- $\kappa$ B p65 were evaluated by in silico analysis, through molecular docking, according to Grancieri et al.<sup>[32]</sup> The tool Instant MarvinSketch (ChemAxon Ltd., <https://www.chemaxon.com>) was used to design the peptides and the AutoDockTools used to merge non-polar hydrogen atoms and define rotatable bonds. The compound 4-Methyl-1-N-(3-phenylpropyl) benzene-1,2-diamine (JSH23) was used as a pharmacological control, as performed by Grancieri et al.,<sup>[32]</sup> aiming to evaluate the peptides interaction in comparison to a compound that has been used as a nuclear factor  $\kappa$ B (NF- $\kappa$ B) p65 inhibitor.<sup>[50]</sup> The crystal structure file of NF- $\kappa$ B p65 (PDB file: 1OY3) was obtained from the Protein Data Bank (<http://www.rcsb.org/>). The Autodock Tools were used to assign flexible torsions, charges, and grid size.<sup>[51]</sup> Docking calculations were performed using AutoDock Vina.<sup>[52]</sup> The binding pose with the highest binding affinity (i.e., lowest binding energy) was then visualized in the Discovery Studio 2016 Client (Dassault Systems Biovia Corp).

**Statistical Analysis:** The results were expressed in bar graphs representing the mean and SEM. The statistical analyses were performed using the statistical package GraphPad Prism 8.0.1 (GraphPad Software, Inc., San Diego, CA, USA), by ANOVA followed by Dunnett’s test to compare the mean of each treatment with the mean of the control. The convention \* $p$  < 0.05, \*\* $p$  < 0.01, \*\*\* $p$  < 0.001, and \*\*\*\* $p$  < 0.0001 was used in the figures. The results for analyses with peptide treatment at different concentrations were also analyzed by ANOVA followed by Tukey’s test for multiple comparisons between each treatment (Table S1, Supporting Information). The results for TNF- $\alpha$  in primary microglia and NF- $\kappa$ B nuclear translocation with peptide treatment at 100  $\mu$ g mL<sup>-1</sup> were analyzed by ANOVA followed by Tukey’s test for multiple comparisons between each treatment.

## Supporting Information

Supporting Information is available from the Wiley Online Library or from the author.

## Acknowledgements

This work was supported by grant # 2019/17269-9 (São Paulo Research Foundation – FAPESP) and by NIH R01 AG059622.

## Conflict of Interest

The authors declare no conflict of interest.

## Author Contributions

M.E.C.S. executed the assays on the project and wrote the main draft of the manuscript; M.E.C.S., L.R., and M.V.R. executed primary microglia and qPCR experiments; R.W.J., L.R., and M.T.B.P. performed critical analysis and scientific guidance throughout the research; R.W.J. also did overall concept and editing of the manuscript. All authors critically revised the manuscript and gave final approval for submission.

## Data Availability Statement

Data available on request from the authors.

## Keywords

food-derived peptides, metal chelation, molecular docking, neuroinflammation, primary microglia

Received: February 19, 2021

Revised: August 12, 2021

Published online: September 28, 2021

- [1] D. M. Norden, J. P. Godbout, *Neuropathol. Appl. Neurobiol.* **2013**, 39, 19.
- [2] M. Prinz, J. Priller, S. S. Sisodia, R. M. Ransohoff, *Nat. Neurosci.* **2011**, 14, 1227.
- [3] J. C. Nissen, *Int. J. Mol. Sci.* **2017**, 18, 561.
- [4] R. W. Johnson, *Brain, Behav., Immun.* **2015**, 43, 1.
- [5] N. L. Sparkman, R. W. Johnson, *NeuroImmunoModulation* **2008**, 15, 323.
- [6] M. Jana, C. A. Palencia, K. Pahan, *J. Immunol.* **2008**, 181, 7254.
- [7] D. G. Walker, J. Link, L. F. Lue, J. E. Dalsing-Hernandez, B. E. Boyes, *J. Leukocyte Biol.* **2006**, 79, 596.
- [8] G. M. Murphy, Jr., L. Yang, B. Cordell, *J. Biol. Chem.* **1998**, 273, 20967.
- [9] C. K. Glass, K. Saijo, B. Winner, M. C. Marchetto, F. H. Gage, *Cell* **2010**, 140, 918.
- [10] M. Prinz, S. Jung, J. Priller, *Cell* **2019**, 179, 292.
- [11] N. M. Rodriguez-Martin, R. Toscano, A. Villanueva, J. Pedroche, F. Millan, S. Montserrat-de la Paz, M. C. Millan-Linares, *Food Funct.* **2019**, 10, 6732.
- [12] M. Grancieri, H. S. D. Martino, E. Gonzalez de Mejia, *Mol. Nutr. Food Res.* **2019**, 63, 1900021.
- [13] J. E. Yuste, E. Tarragon, C. M. Campuzano, F. Ros-Bernal, *Front. Cell. Neurosci.* **2015**, 9, 322.
- [14] M. A. Lovell, J. D. Robertson, W. J. Teesdale, J. L. Campbell, W. R. Markesbery, *J. Neurol. Sci.* **1998**, 158, 47.
- [15] M. Manto, *Toxics* **2014**, 2, 327.
- [16] X. Tan, Y. Zhou, P. Gong, H. Guan, B. Wu, L. Hou, X. Feng, W. Zheng, J. Li, *J. Trace Elem. Med. Biol.* **2019**, 52, 199.
- [17] S. A. James, I. Volitakis, P. A. Adlard, J. A. Duce, C. L. Masters, R. A. Cherny, A. I. Bush, *Free Radic. Biol. Med.* **2012**, 52, 298.
- [18] G. Rathnasamy, E. A. Ling, C. Kaur, *CNS Neurol. Disord. Drug Targets* **2013**, 12, 785.
- [19] M. Sastre, C. W. Ritchie, N. Hajji, J. S. M. Alzheimer’s, *Dis. Relat. Dement* **2015**, 2, 1014.
- [20] M. Jureschi, A. V. Lupaescu, L. Ion, B. A. Petre, G. Drochioiu, *Adv. Exp. Med. Biol.* **2019**, 1140, 401.

- [21] Y. Liu, M. Nguyen, A. Robert, B. Meunier, *Acc. Chem. Res.* **2019**, *52*, 2026.
- [22] C. Rodríguez-Rodríguez, M. Telpoukhovskaia, C. Orvig, *Coord. Chem. Rev.* **2012**, *256*, 2308.
- [23] L. Guo, P. A. Harnedy, B. Li, H. Hou, Z. Zhang, X. Zhao, R. J. FitzGerald, *Trends Food Sci. Technol.* **2014**, *37*, 92.
- [24] F. G. D. e Silva, L. N. Paiatto, A. T. Yamada, F. M. Netto, P. U. Simioni, W. M. S. C. Tamashiro, *Mol. Nutr. Food Res.* **2018**, *62*, 1800088.
- [25] E. G. de Mejia, V. P. Dia, *Peptides* **2009**, *30*, 2388.
- [26] B. Qian, X. Zhao, Y. Yang, C. Tian, *Food Sci. Nutr.* **2020**, *8*, 3947.
- [27] D. Ren, P. Wang, C. Liu, J. Wang, X. Liu, J. Liu, W. Min, *J. Funct. Foods* **2018**, *46*, 449.
- [28] Y. Ma, J. Liu, H. Shi, L. L. Yu, *J. Dairy Sci.* **2016**, *99*, 6902.
- [29] A. F. Piccolomini, M. M. Iskandar, L. C. Lands, S. Kubow, *Food Nutr. Res.* **2012**, *56*.
- [30] M. Dadar, Y. Shahali, S. Chakraborty, M. Prasad, F. Tahoori, R. Tiwari, K. Dhama, *Inflammation Res.* **2019**, *68*, 125.
- [31] M. E. Caetano-Silva, F. Moreira Simabuco, R. Maria Neves Bezerra, D. Cristina da Silva, E. Alves Barbosa, D. Carneiro Moreira, G. Dotto Brand, J. R. d. S. d. A. Leite, M. T. B. Pacheco, *J. Agric. Food Chem.* **2020**.
- [32] M. Grancieri, H. S. D. Martino, E. Gonzalez de Mejia, *Food Chem.* **2019**, *289*, 204.
- [33] N. Lannes, E. Eppler, S. Etemad, P. Yotovskii, L. Filgueira, *Oncotarget* **2017**, *8*, 114393.
- [34] S. Guha, K. Majumder, *J. Food Biochem.* **2019**, *43*, e12531.
- [35] L. Mojica, D. A. Luna-Vital, E. González de Mejía, *J. Sci. Food Agric.* **2017**, *97*, 2401.
- [36] S. Chakraborti, F. Jahandideh, J. Wu, *Biomed Res. Int.* **2014**, *2014*, 11.
- [37] B. Stansley, J. Post, K. Hensley, *J. Neuroinflammation* **2012**, *9*, 115.
- [38] A. Kumar, G. Negi, S. S. Sharma, *Biochimie* **2012**, *94*, 1158.
- [39] E. C. Dresselhaus, M. K. Meffert, *Front. Immunol.* **2019**, *10*, 1043.
- [40] V. Pande, R. K. Sharma, J.-I. Inoue, M. Otsuka, M. J. Ramos, *J. Comput.-Aided Mol. Des.* **2003**, *17*, 825.
- [41] V. Mukund, S. K. Behera, A. Alam, G. P. Nagaraju, *Bioinformatics* **2019**, *15*, 11.
- [42] S. Fujioka, J. Niu, C. Schmidt, G. M. Sclabas, B. Peng, T. Uwagawa, Z. Li, D. B. Evans, J. L. Abbruzzese, P. J. Chiao, *Mol. Cell. Biol.* **2004**, *24*, 7806.
- [43] F. Aktan, *Life Sci.* **2004**, *75*, 639.
- [44] Y. Ano, Y. Yoshino, T. Kutsukake, R. Ohya, T. Fukuda, K. Uchida, A. Takashima, H. Nakayama, *Aging* **2019**, *11*, 2949.
- [45] Y. Ano, T. Ayabe, T. Kutsukake, R. Ohya, Y. Takaichi, S. Uchida, K. Yamada, K. Uchida, A. Takashima, H. Nakayama, *Neurobiol. Aging* **2018**, *72*, 23.
- [46] Y. Ano, R. Ohya, Y. Takaichi, T. Washinuma, K. Uchida, A. Takashima, H. Nakayama, *J. Alzheimer's Dis.* **2020**, *73*, 1331.
- [47] J. Adler-Nissen, *Enzymic Hydrolysis of Food Proteins*, Elsevier applied science publishers, **1986**.
- [48] M. Nikodemova, J. J. Watters, *J. Neuroinflammation* **2012**, *9*, 147.
- [49] O. J. Trask Jr, *Assay Guidance Manual [Internet]*, Eli Lilly & Company and the National Center for Advancing Translational Sciences, **2012**.
- [50] Q. Wang, X. Dong, N. Li, Y. Wang, X. Guan, Y. Lin, J. Kang, X. Zhang, Y. Zhang, X. Li, T. Xu, *Pharmacol. Biochem. Behav.* **2018**, *169*, 59.
- [51] G. M. Morris, R. Huey, W. Lindstrom, M. F. Sanner, R. K. Belew, D. S. Goodsell, A. J. Olson, *J. Comput. Chem.* **2009**, *30*, 2785.
- [52] O. Trott, A. J. Olson, *J. Comput. Chem.* **2010**, *31*, 455.